This is a repository copy of *Design and Properties of Novel Substituted Borosilicate Bioactive Glasses and Their Glass-Ceramic Derivatives*.

White Rose Research Online URL for this paper:
http://eprints.whiterose.ac.uk/102225/

Version: Accepted Version

The Design and Properties of Novel Substituted Borosilicate Bioactive Glasses and Their Glass-Ceramic Derivatives

João S. Fernandes[1,3], Piergiorgio Gentile[2], Robert Moorehead[2], Aileen Crawford[2], Cheryl Miller[2], Ricardo A. Pires[1,3,*], Paul V. Hatton[2,*], Rui L. Reis[1,3]

[1] 3B's Research Group - Biomaterials, Biodegradables and Biomimetics, University of Minho, Headquarters of the European Institute of Excellence on Tissue Engineering and Regenerative Medicine, Parque da Ciência e Tecnologia, Zona Industrial da Gandra, 4805-017 Barco, GMR, Portugal

[2] Bioengineering and Health Technologies Research Group, School of Clinical Dentistry, University of Sheffield, Claremont Crescent, Sheffield S10 2TA, United Kingdom

[3] ICVS/3B's - PT Government Associate Laboratory, Braga/Guimarães, Portugal

* Corresponding Authors:

Ricardo A. Pires. E-mail: rpires@dep.uminho.pt

Tel: +351 253 510 907

Fax: +351 253 510 909

and

Prof Paul V. Hatton. E-mail: paul.hatton@sheffield.ac.uk

Tel: +44 (0) 114 271 7938

Fax: +44 (0) 114 226 5484

1   **Abstract**

2   Three novel borosilicate bioactive glasses (BBGs) of general formula of $0.05Na_2O \cdot 0.35x$

3   $\cdot 0.20B_2O_3 \cdot 0.40SiO_2$ (molar ratio, where x = MgO or CaO or SrO) were prepared and used to

4   investigate the effect of crystallisation on their properties including cytotoxicity. The three post-

5   melt compositions were determined using X-ray fluorescence spectroscopy and crystallisation

6   events were studied using differential thermal analysis and x-ray diffraction. This information was

7   used to determine heat treatments to prepare glass-ceramics by controlled crystallisation. X-ray

8   diffraction analysis and Fourier transform infrared spectroscopy showed that, after higher heat

9   treatment temperatures (800-900 ºC), borosilicate bioactive glass-ceramics (BBGCs) contained

10 mainly borate and silicate crystalline phases. Specifically, BBG-Mg, BBG-Ca and BBG-Sr glass-

11 ceramics detected the presence of magnesium silicate-$Mg_2(SiO_3)_2$ and magnesium borate-$Mg_2B_2O_5$;

12 wollastonite-2M-$CaSiO_3$ and calcium borate-$Ca(BO_2)_2$; and strontium silicate-$SrSiO_3$ and strontium

13 borate-$Sr_2B_2O_5$, respectively. In vitro cytotoxicity tests were performed using the mouse fibroblast

14 cell line (L929). Glass and glass ceramic at concentrations lower than 50 mg/ml did not exhibit any

15 level of cytotoxicity when compared with the control. However, quantitative evaluation indicated

16 that greater cell growth occurred in the presence of materials with crystalline phases. Control of

17 BBGs crystallisation may therefore be used to influence the biocompatibility of these glass-ceramic

18 systems.

19 **Keywords:** Bioactive glasses, borosilicate, crystallisation, glass-ceramic and cytotoxicity.

1. Introduction

Bioactive glasses (BGs) and bioactive glass-ceramics (BGCs) have been evaluated for a wide range of clinical applications related to bone tissue repair and regeneration [1]. BGs and BGCs are widely reported to form a bone-like hydroxyapatite (HA) layer on their surface when placed in a simulated biological environment [2]. This has also been demonstrated to occur in vivo [3]. Formation of a bone-like HA layer is a fundamental requirement for the establishment of a strong interfacial bond between implants and bone [4]. Since Hench et al. [2] proposed the $CaO: SiO_2: Na_2O: P_2O_5$ system in 1969, 45S5 bioglass (or Bioglass®) has become the gold standard for this type of material. However, slow degradation rate is a major disadvantage of the silicate based BG, which makes it difficult to match the degradation rate of the BG scaffolds with the rate of new tissue formation [5,6]. Moreover, some studies with silicate glasses report slow conversion rate to a bone-like HA and often this conversion remains incomplete. Therefore unconverted glass containing SiO_2 could remain in human body long after its implantation, raising uncertainty regarding the long-term effects of SiO_2 in vivo [7,8].

The addition of boron oxide to the glass network is one approach that has the potential to overcome the limitations identified above by modifying dissolution rates as well as other properties including tissue bonding [9]. The incorporation of boron in a silicate glass matrix involves lower melting temperatures, with an increased bio-degradation and increased conversion to HA [8,10,11]. Furthermore, boron is reported to be beneficial for bone healing and its controlled release stimulates bone formation and maintenance. Frequently, it has been associated with the increase in bone resistance to fractures [12-14]. Thereby, borosilicate bioactive glasses (BBGs) composition may be used to achieve a more controlled release of specific component ions in order to trigger a range of biological responses [15]. Control of the surface reactions and therefore of the biodegradation and bioactivity of implanted materials can be achieved by varying the chemical nature and/or

concentration of the BBGs constituents. For instance, Ciceo Lucacel et al. [16] have used the calcium BBGs doped with silver (Ag^+) to better control Ag^+ antibacterial properties. Xu et al. [6] have also proposed a sol–gel-derived calcium BBGs system for reinforcing glass-ceramic porous biomaterials and accurately control theirs biodegradability. In another study by Wang et al. [17], evaluating the of osteogenic properties of BBGs doped with Zinc (Zn^{2+}) these BBGs significantly enhanced bone regeneration in bone defects when implanted into the rats in vivo. Baiano et al. [18] used bioactive glass-based trabecular coating for the development of a novel prosthetic acetabular cup to have an improved in vivo interfacial bond with bone.

While studies have been demonstrating the ability of BBGs to better control degradation, thus increasing the beneficial properties of ions release, there are still concerns regarding toxicity when those glasses are implanted [19, 20]. There are several metal ions that at higher concentrations are extremely toxic. In particular, boron release has been associated with cell growth inhibition for concentrations greater then 2.5 mM and also causes cytotoxicity due to release of $(BO_3)^{3-}$ into the medium [12, 19, 20]. Several cellular studies investigated the cytotoxicity of BGs and reported inhibition of cell viability and proliferation for high doses of ions in culture [21, 22]. For instance, Santocildes-Romero et al. [23] have showed an increase of the cytotoxic effect of BGs dissolution by increasing the amount of glass powders used and the level of strontium substitution added to the glass composition. Moreover, specific component ions released in a controlled rate may stimulate differently cells. Metallic ions such as magnesium (Mg^{2+}), calcium (Ca^{2+}) or strontium (Sr^{2+}) can stimulate bone cell proliferation, differentiation and extracellular matrix mineralisation, as well as increase the production rate of HA and bone [21, 22, 24-26]. For instance, Mg^{2+} in commonly related with cells adhesion and stability [24], while Ca^{2+} [25] and Sr^{2+} [26] are generally associated to apatite formation process and cells differentiation and mineralisation. Moreover, Sr^{2+} has been successfully studied for the treatment of osteoporosis [21].

Various studies have been reported concerning the use of heat treatments in order to induce crystallisation in BGs to promote changes in their physico-chemical properties [27-31]. For instance,

Rao et al. [32] have observed improvements in the dielectric constant and less dielectric loss of sodium borosilicate glasses ($SiO_2 - B_2O_3 - Na_2O$ system) with increase in the duration of the heat treatment. Daguano et al. [27] developed and characterised BGs and BGCs from the $CaO-P_2O_5-SiO_2-MgO$ system, using different degrees of crystallinity. They showed that partial crystallisation improved mechanical properties by phase transformation, which modified the microstructure of the base glassy material. Therefore, after studying the thermal profile of BGs, appropriated heat treatment cycle with a controlled temperature increase could be applied to promote the re-arrangement of the glass structures generating a well-ordered and crystalline structure. The properties of the formed glass-ceramics are mostly influenced by the characteristics of the finely dispersed crystalline and the residual glassy phases, which can be controlled by the composition of the base glass. However, few authors have reported that the formation of new crystalline phases provoked the modification of toxic effects induced by the glasses in cells [27, 30]. Specially, Hurrell-Gillingham et al. [30] investigated the effects of devitrification of glass-ionomer cements (GICs) from $SiO_2-Al_2O_3-P_2O_5-CaO-CaF_2$ system on glass-ceramic formation and in vitro biocompatibility. They demonstrated that crystallisation might be used to improve the in vitro biocompatibility of GICs. Also Freeman at al. [33] studied the response to implantation of apatite glass-ceramics. They demonstrated that crystallisation significantly improved the bone tissue response.

It seems likely that devitrification of glasses represents a route to modify and study their properties including biocompatibility. However, few attempts to modify the biocompatibility of a medical grade glasses using this approach have been reported [30, 33]. This study aimed to firstly synthesise and characterise the thermal and chemical properties of three novel substituted BBGs. The incorporation of different ions (i.e. Mg^{2+}, Ca^{2+} and Sr^{2+}) in BBGs lies on the fact that specific effects can be used to achieve different human cell behaviour by the release of ionic dissolution products. Secondly, we aimed to investigate the effect of BBGs crystallisation on their cytotoxic effects, providing a method for the improvement of bioactive borosilicate glass-ceramics cellular properties.

2. Materials and methods

2.1. Materials

All chemical compounds used for melt-quenched synthesis were reagent grade: di-boron trioxide (Alfa Aesar, Germany), calcium carbonate (Sigma-Aldrich, Portugal), sodium bicarbonate (Sigma-Aldrich, Australia), silica gel 60M (Macherey-Nagel, Germany), magnesium oxide (Sigma-Aldrich, Portugal) and strontium carbonate (Sigma-Aldrich, Australia).

2.2. Glass synthesis and preparation

The novel BBGs of general formula $0.05Na_2O \cdot xMgO \cdot yCaO \cdot (0.35\text{-x-y})SrO \cdot 0.20B_2O_3 \cdot 0.40SiO_2$ (molar ratio, where x, y = 0.35 or 0.00, and x ≠ y) were synthesised by melt quenching. The appropriate amounts of SiO_2, B_2O_3, $NaHCO_3$, and $CaCO_3$ or MgO or $SrCO_3$ were accurately mixed with ethanol (Sigma, Portugal) in a porcelain pestle and mortar, fully dried overnight and transfer to a platinum crucible. The batch was heated to 1450 ˚C in air for 1 hour and subsequently the melt was quickly poured in a water bath at 4 ˚C to form a glass frit. The glass frit was ground into an Agate mortar (RETSCH, Germany) to obtain microparticles and then, sieved for a size smaller than 63 μm.

2.3. Characterisation

2.3.1. X-ray fluorescence (XRF)

The X-ray fluorescence spectroscopy was used to confirm the glass composition (Philips PW2400 X-ray fluorescence spectrometer). Samples were prepared by fusing powdered glass with a known quantity of boron and a flux producing a glass-like bead. After which, they were irradiated with high-energy primary X-ray photons. All the samples were run in triplicate and the percentage (w/w) of the oxides present were determined. Afterwards, molar percentage was calculated for all the samples.

1   2.3.2. Differential thermal analysis (DTA) and heat treatment

2   The mid point of glass transition (T_g), and crystallisation (T_c) temperatures were determined by

3   differential thermal analysis (Perkin-Elmar DTA7 running Pyris thermal analysis software in Unix)

4   at a heating rate of 10 °C min^{-1} from 50 to 1300 °C.

5   In accordance with DTA data, crystallised glass was prepared for each sample. Briefly, fast-

6   quenched particles of the glass samples were heat-treated with a heating rate of 10 °C min^{-1} and

7   held for 120 min at each temperature (T_g, T_{c1}, T_{c2} and T_{c3}) before cooling to room temperature.

8   2.3.3. X-ray diffraction analysis (XRD) and attenuated total reflection Fourier transform

9   infrared (ATR-FTIR) spectroscopy

10   The glasses were analysed before and after each heat treatment by X-ray diffraction analysis (XRD)

11   and attenuated total reflection Fourier transform infrared spectroscopy (ATR-FTIR). A STOE

12   STADI P X-ray diffractometer was used to identify the crystalline phases. The glass samples were

13   place in aluminium holders and analysed by Cu radiation of wavelength 1.5406 Å at 40 kV and 40

14   mA with a step size of 0.2° in a range of 2θ values from 10° to 80° at a scanning speed of 10 s/step.

15   The crystalline patterns were identified by the use of the cards listed in the Joint Commission on

16   Powder Diffraction Standards (JCPDS). The ATR-FTIR spectra were obtained using a Perkin-

17   Elmer GX instrument in the range of 4000-550 cm^{-1} (resolution 4 cm^{-1}) for the identification of the

18   chemical bonds present in the glass or glass-ceramic structures.

19   **2.4. In vitro cytotoxicity**

20   The in vitro cytotoxicity study was design following the international guidelines ISO 10993-5:2009

21   [34], using immortalised mouse lung fibroblast-like cell line (L929, Rockville, MD) in indirect contact

22   with glass powders for 3 days. The samples were sterilised in an oven (Gallenkamp Hot Box,

23   England) at 160 °C for 120 min. After sterilisation, the glasses were added to Dulbecco's modified

24   Eagle medium (DMEM, Sigma-Aldrich, UK) solution at a concentration of 0.2 g/mL and incubated

1   for 24 h at 37 °C. After incubation, the glass-conditioned medium was removed and filtered through

2   a 0.2 µm membrane.

3   The L929 cells were expanded in DMEM supplemented with 10 % (v/v) fetal calf serum (Sigma-

4   Aldrich, UK), penicillin (100 U/mL, Sigma-Aldrich, UK) and streptomycin (100 µg/mL, Sigma-

5   Aldrich, UK), and non-essential amino acids (NEAA, Sigma-Aldrich, UK). The L929 cells were

6   cultured at 37 °C in an atmosphere of 5 % CO_2. Confluent L929 cells at passages between 15 and

7   19 were harvested and seeded into 48-well culture plates (growth area 0.95 cm^2) at a density of

8   2×10^4 cells/well. After a 24 h culture period the culture media was discarded and replaced with 0.5

9   cm^3 of serially diluted, glass-conditioned medium (at a final concentrations of 100, 50, 25, 10, and 5

10   %). L929 cells cultured in the absence of glass particles, was used as negative control and 45S5

11   bioglass- conditioned medium as positive control. After 1 and 3 days time of culturing, the culture

12   medium was removed and the viability and DNA content of the cultures were analysed using

13   PrestoBlue® and Picogreen® assays respectively.

14   **Cell viability assessment:** The PrestoBlue® reagent (Fisher Scientific, UK) is a resazurin-based

15   non-fluorescent solution that is reduced to fluorescent resorufin by viable cells. The assay was

16   performed according to the manufacturer's instructions. In brief, the PrestoBlue® reagent was added

17   to a final concentration of 10% to the cell cultures and the cultures incubated for 1 h at 37°C. 200 µl

18   samples of the culture medium were removed and placed in 96-well plates and the resorufin

19   fluorescence quantified spectrophotometrically using a plate reader (Tecan Infinite M200). The

20   fluorescence was determined at an excitation wavelength of 560 nm and emission wavelength of

21   590 nm. The cell viabilities are normalised as % of the metabolic activity of the control cell

22   cultures.

23   **DNA measurement:** The PicoGreen® dsDNA reagent (Invitrogen, USA) is an ultrasensitive

24   fluorescent nucleic acid dye for quantification of double-stranded DNA (dsDNA) in solution. This

25   assay enables measurement of cell proliferation. After each culturing period, the cell monolayers

were washed with PBS and then incubated at 37 ℃ for 3 h followed by freezing step at -80 ℃ for at

least over night in ultra-pure water (1 mL) to ensure cell lysis. The assay was performed according

to the manufacturer's protocol. And the fluorescence was determined at an excitation wavelength

of 485 nm and emission wavelength of 528 nm. The DNA values were normalised to those of the

control cultures

Morphological evaluation of cell cultures: After each culturing period the cell monolayers were

washed with PBS and fixed with 4 % formalin solution (0.5 mL) for 15 min at room temperature

(RT). The cell layers were then washed with PBS, containing 0.2 % Triton X, for 2 min. After the

fixation and permeation steps, the cell monolayers were washed again with PBS and stained with

4,6-diamidino-2-phenyindole dilactate (1:1000 DAPI, Sigma, UK) for 2 min at RT, and phalloidin-

tetramethylrhodamine B isothiocyanate (Sigma, UK) for 1 h at RT. Finally, the cells were washed

and observed using an Axioplan 2 imaging fluorescent microscope with a digital camera QIC AM

12-bit (Zeiss, UK).

2.5. Statistical analysis

Experiments were run at least in triplicate for each sample. All data were expressed as mean ±

standard deviation (SD). Statistical analysis was determined by using Graphpad Prim® software,

version 6.0. The normality of the data distribution was monitored by Shapiro-Wilk test ($p < 0.05$).

Some of the datasets were not considered to have a normal distribution, requiring a non-parametric

statistical evaluation. In this context, Kruskal-Wallis test ($p < 0.05$) was applied to all dataset,

followed by a Dunn's Multiple Comparison test.

3. Results and Discussion

3.1. Glass characterisation

3.1.1. X-ray fluorescence

The X-ray fluorescence data, presented in Table 1, confirmed that the experimental compositions of bioactive borosilicate glasses obtained by melt-quench method were close to the expected theoretical composition, indicating that the glass network structure was formed as aimed. However, the slight differences between theoretical and XRF data may have been caused by the high volatility of alkali-borate compounds during melting process [35].
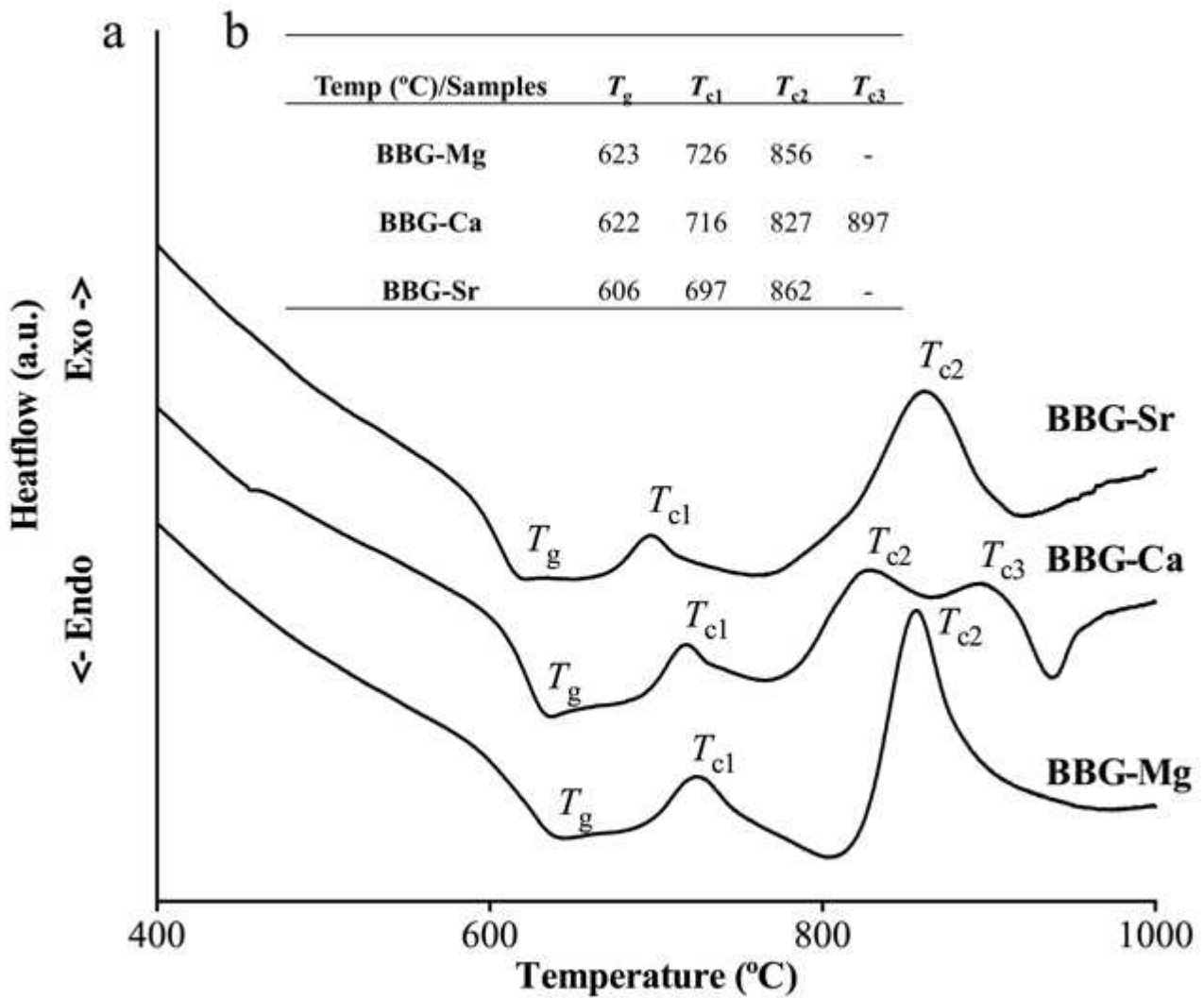
Table 1 - X-ray fluorescence spectrometry estimation of elemental concentration (mol %) of BBGs. BBG-Mg, -Ca and -Sr glasses (* varies with the specific ion for each glass). All analysis were performed in triplicate and standard deviation < 0.05.

Samples / composition	Si (mol %)	B (mol %)	Na (mol %)	Ions* (mol %)
BBG-Mg	37.6 (40)	34.8 (40)	10.4 (10)	39.7 (35)
BBG-Ca	36.9 (40)	43.8 (40)	10.4 (10)	36.0 (35)
BBG-Sr	37.5 (40)	41.4 (40)	10.4 (10)	36.7 (35)

3.1.2. Differential thermal analysis

The DTA was used to study the phase transformation temperatures of the BBGs in order to determine the heat treatment schedule. DTA patterns from all BBGs are presented in Figure 1a. For BBG-Mg and BBG-Sr along with the mid point of glass transition temperature (T_g - endothermic peak), two crystallisation temperatures (T_c - exothermic peaks) were found; while BBG-Ca glasses presented a T_g and one exothermic (T_{c1}) peak followed by a doublet exothermic peak (T_{c2} and T_{c3}).

1 The T_g and T_c used for the different glass compositions are listed in Figure 1b. The BBGs revealed

2 crystallisation temperatures within the range of temperatures of 700 to 900 °C with two phases

3 frequently related with borate and silicate crystal phases [15]. The endothermic peaks are related to

4 the molecular re-arrangement in glass structure preceding and during glass crystallisation, a process

5 known for crystal nucleation and growth [15, 29]. In order to induce crystal nucleus formation in the

6 glass structure, BBGs were kept for 2 hours at T_g and subsequently for 2 hours at each T_c. Each

7 well-defined exothermic peak may result in the formation of a different crystalline phases [28]. For

8 each BBGs different heat treatment schedules were applied according to the endo- and exothermic

9 peak temperatures reported in Figure 1b.

Temp (°C)/Samples	T_g	T_{c1}	T_{c2}	T_{c3}
BBG-Mg	623	726	856	-
BBG-Ca	622	716	827	897
BBG-Sr	606	697	862	-

10

11 **Figure 1** - (a) DTA patterns of BBG-Mg, BBG-Ca and BBG-Sr glasses. T_g – mid point of glass

12 transition temperature and T_c – crystallization temperature. (b) The mid point of glass transition

1 temperature and crystallization temperatures for the BBGs (BBG-Mg, -Ca and -Sr glasses)

2 determined by DTA analysis (T_g – mid point of glass transition temperature and T_c – crystallization

3 temperature).

4   3.1.3. X-ray diffraction and attenuated total reflection Fourier transform infrared

5 The XRD analysis was performed in order to study the crystallinity of the glasses before and after

6 heat treatments and the respective phases formed (Table 2). Figure 2a, 2b and 2c shows the phase

7 evolution XRD patterns of BBG-Mg, -Ca and -Sr glasses, respectively, from amorphous to

8 crystalline phase after the different heat treatment schedules. Heat treatment schedule at T_g were

9 performed and exhibit no significant difference in respect with the as quenched XRD patterns.

10 The XRD patterns of BBG-Mg glass after the first crystallisation heat treatment (BBG-Mg_T_{c1})

11 showed a predominantly amorphous phase with weak diffraction peaks, which can be assigned to

12 silicon oxide (SiO_2, JCPDS Card No. 11-252). After T_{c2} heat treatment (BBG-Mg_T_{c2}) two

13 predominant crystalline phases of magnesium silicate ($Mg_2(SiO_3)_2$, JCPDS Card No. 86-433) and

14 magnesium borate ($Mg_2B_2O_5$, JCPDS Card No. 73-2232) were observed.

15 In the case of XRD patterns of BBG-Ca glass after the first crystallisation heat treatment (BBG-

16 Ca_T_{c1}) it was observed a predominantly amorphous phase with some weak diffraction peaks,

17 which can be attributed either to calcium silicate ($CaSiO_3$, JCPDS Card No. 76-186) and/or calcium

18 borate ($Ca(BO_2)_2$, JCPDS Card No. 31-155), indicating that after T_{c1} crystallisation started to occur.

19 After the second heat treatment (BBG-Ca_T_{c2}) there is the formation of two predominant crystalline

20 phases, calcium silicate, commonly referred as wollastonite-2M and calcium borate. After the T_{c3}

21 heat treatment (BBG-Ca_T_{c3}) the diffraction patterns are comparable to the previous heat treatment

22 patterns (T_{c2}), which indicates that no detectable amount of different crystalline phase is forming.

23 For the BBG-Sr glass, after the first crystallisation heat treatment (BBG-Sr_T_{c1}) it was observed a

24 predominant amorphous phase of the glass and a weak diffraction peak, in which the weak peaks

can be attributed either to strontium silicate ($SrSiO_3$, JCPDS Card No. 87-474) and/or strontium borate ($Sr_2B_2O_5$, JCPDS Card No. 19-1268), suggesting that the formation of crystalline phases starts after the first crystallisation heat treatment. After the second heat treatment (BBG-Sr_T_{c2}) there were formed two crystalline phases of strontium silicate and strontium borate.

Finally, XRD data showed that for all BBGs after heat treatment with lower crystallisation temperatures (T_{c1}) there was predominantly amorphous with only a small amount crystals formation. However after latter heat treatments (T_{c2} and T_{c3}) occurred the formation of crystalline phases resulting in new silicate and borate glass-ceramics.

Table 2 - Crystalline phases of BBG-Mg, -Ca and -Sr glasses obtained after heat treatments

| Heat treatment	Heat temperature conditions	Crystalline phases
BBG-Mg_T_{c1}	623 °C / 2h + 726 °C / 2 h	Glass and SiO_2
BBG-Mg_T_{c2}	623 °C / 2 h + 856 °C / 2 h	$Mg_2(SiO_3)_2$; $Mg_2B_2O_5$
BBG-Ca_T_{c1}	622 °C / 2 h + 716 °C / 2 h	Glass and $Ca(BO_2)_2$
BBG-Ca_T_{c2}	622 °C / 2 h + 827 °C / 2 h	$CaSiO_3$; $Ca(BO_2)_2$
BBG-Ca_T_{c3}	622 °C / 2 h + 897 °C / 2 h	$CaSiO_3$; $Ca(BO_2)_2$
BBG-Sr_T_{c1}	606 °C / 2 h + 697 °C / 2 h	Glass and $SrSiO_3$; $Sr_2B_2O_5$
BBG-Sr_T_{c2}	606 °C / 2 h + 862 °C / 2 h	$SrSiO_3$; $Sr_2B_2O_5$
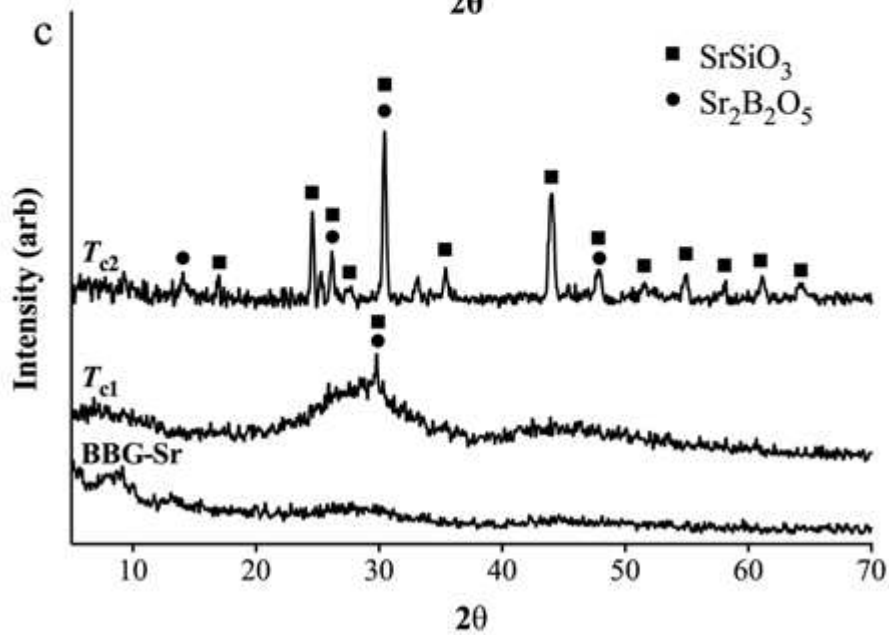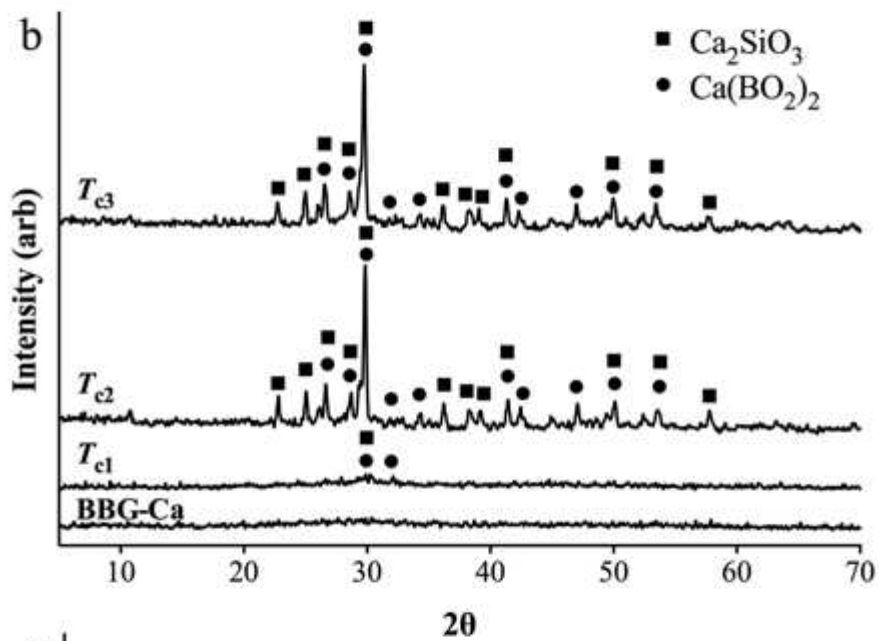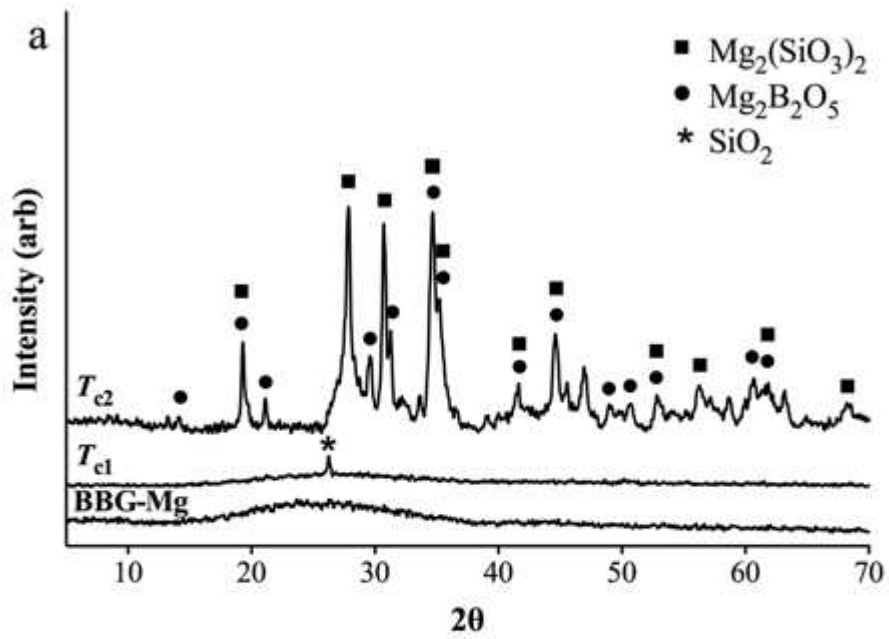
1 **Figure 2** - X-ray diffraction patterns of phase evolution over increasing crystallisation temperatures

2 for BBG-Mg (a), -Ca (b), -Sr (c) glasses (BBG-ion - before heat treatment, T_{c1} - after first heat

3 treatment, T_{c2} - after second heat treatment, T_{c3} - after third heat treatment).

4 The ATR-FTIR analysis was performed to evaluate the possible changes of vibrational spectra after

5 the heat treatments, because they can induce a process of structural grouping re-arrangements,

6 implying important modifications in the properties of the glasses [30, 36]. ATR-FTIR spectra of BBG-

7 Mg, -Ca, -Sr glasses and glass-ceramics are presented in Figure 3a, 3b and 3c, respectively. ATR-

8 FTIR spectra of all BBGs consist of dominant broad bands from 740-585 and 1210-740 cm^{-1}

9 generally attributed to B-O stretching of tetrahedral $[BO_4]$ units, and 1550-1260 cm^{-1}, which are

10 attributed to B-O stretching of trigonal $[BO_3]$ unit [10, 36]. On the other hand the same broad bands

11 from 740-585 and 1240-740 cm^{-1} can be also assigned to Si-O-Si symmetric and asymmetric

12 stretching, respectively [37-39]. The presence of these intense bands indicates the coexistence of

13 silicate and borate bonds, which supports the presence of borosilicate network structure in the

14 amorphous phase. There are two additional less intense bands ranging from 3000 to 2800 and 3750

15 to 3500 cm^{-1} in all spectra before and after heat treatment, which can be associated with water

16 content. The bands in the range 3000 to 2800 cm^{-1} have origin in hydrogen bonds and peaks from

17 3750 to 3500 cm^{-1} are due to OH- groups [36, 40, 41]. Furthermore, there are no significant differences

18 comparing ATR-FTIR spectra of BBGs before and after T_{c1} heat treatment (comparing BBG-ion

19 with T_{c1} of Figure 3a, 3b and 3c). This fact suggests that there was no formation of detectable

20 crystalline phases. However, for the latter heat treatments (T_{c2} and T_{c3}) all BBGs showed a splitting

21 of the intense broad bands in several sharp peaks. The splitting of the broad bands might indicate

22 structural grouping re-arrangements (e.g. 1210-740 cm^{-1} broad band is splitting in 4 different peaks

23 for BBG-Mg glass-ceramic; Figure 3a). Thus, temperatures higher than 800 °C indeed affected the

24 glass network by rearranging the borosilicate structure. Moreover ATR-FTIR spectra of BBG-Ca

25 glass-ceramics (after T_{c2} and T_{c3} heat treatment – Figure 3b) did not show significant differences.

26 This analysis agrees with XRD data, indicating that the crystallisation temperatures of the double

15

exothermic peak found by DTA (Figure 1) did not introduce an evident different molecular re-arrangement in glass structure and thereby theirs ATR-FTIR spectra will be analysed as one. The correspondent assignments for sharp peaks formed after the latter heat treatments (T_{c2} and T_{c3}) are presented in Figure 3d, from where vibrational peaks ranging from 636-595 and 1270-1010 cm^{-1} can be attributed to the formation of Si-O-Si bonds and Si-O-Si asymmetric stretching, respectively [37, 39, 42]. On the other hand peaks ranging from 735-680 and 1010-935 cm^{-1} can be assigned to bending of B_2-O bonds in the borate glassy network and B_2-O bond of tetrahedral [BO_4] [36, 43, 44]. Finally, peaks ranging from 680-645 and 1195-1010 cm^{-1} can be attributed to the formation of Si-O-B bonds [10, 36, 45]. These assigned peaks confirmed the existence of new silicon and boron units at the structure network as shown by XRD data. Of highlighting are the peaks found from 915-830 and 955-870 cm^{-1} that can be assigned to the formation of Si–O–Ion and B-O-Ion bonds. That indicates the presence of silicate and borate structures bonding metallic ions, which is in agreement with the formation of metal silicates and borates found by XRD analysis [10, 42, 43].

The ATR-FTIR analysis showed that for the latter heat treatments there are peaks that can be attributed to B-O-B and Si-O-Si bonds formation. The presence of those bonds supports the formation of silicate and borate crystalline phases previously indicated by XRD data. Also, peaks in the region of 950 to 850 cm^{-1} that are related with the formation either of Ion-O-Si and Ion-O-B, strongly supports the presence of crystalline phases metal silicate and borate.
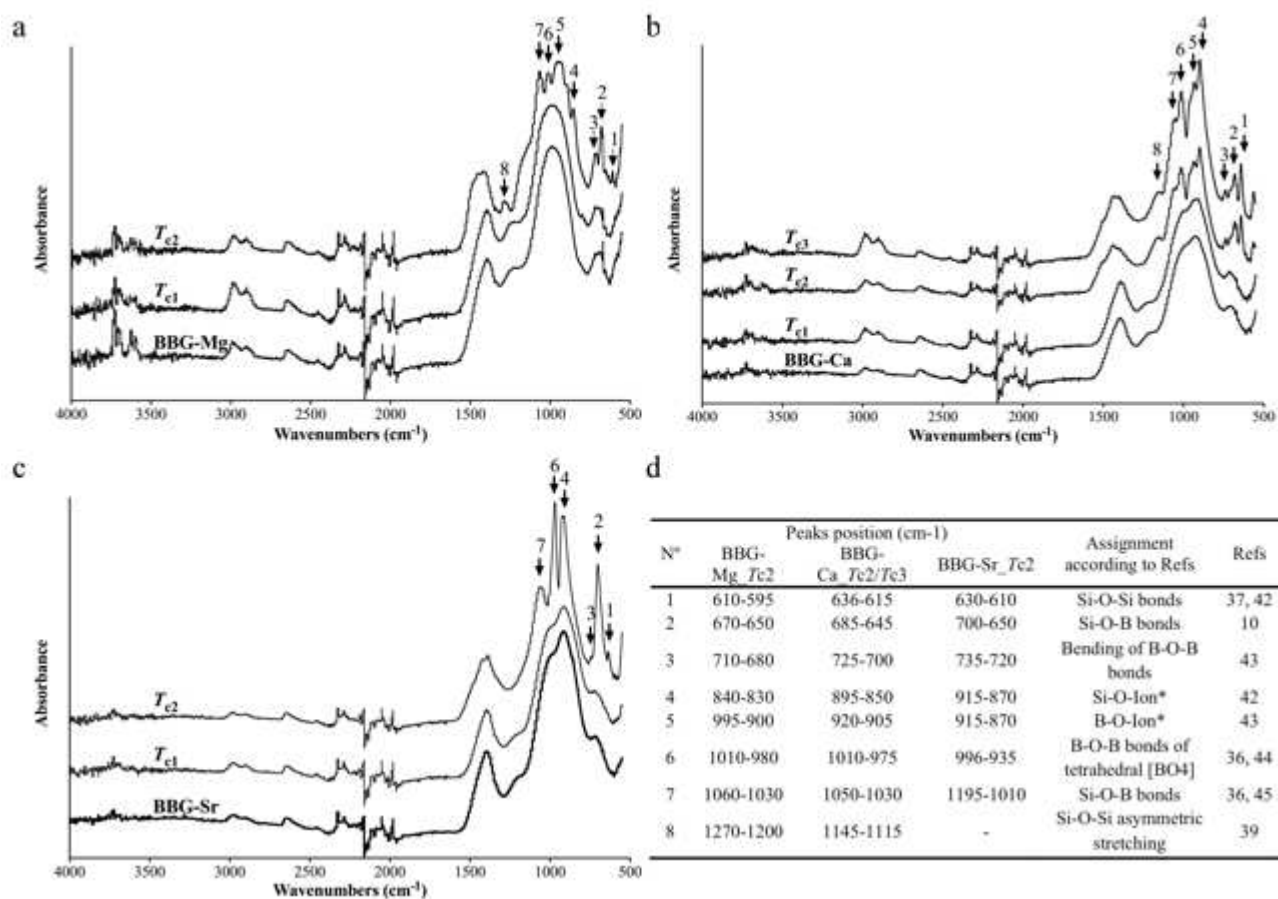
Figure 3 - ATR-FTIR spectra of BBG-Mg (a), -Ca (b) and -Sr (c) glasses (BBG-ion - before heat treatment, T_{c1} - after first heat treatment, T_{c2} - after second heat treatment, T_{c3} - after third heat treatment). The numbers are referred to the type of bond found: 1 and 8 – Si-O-Si; 2 and 7 – Si-O-B; 3 and 6 – B-O-B; 4 – Si-O-Ion; 5 – B-O-Ion. (d) ATR-FTIR band assignments.

3.2. In vitro cytotoxicity

The cytotoxicity studies were designed to evaluate whether the degradation or dissolution of glasses and glass-ceramics affected the viability and proliferation of mouse lung fibroblast-like cells (L929). The experimental design was based on the international guidelines of ISO 10993-5:2009 with some adjustments as described in the methods section [34]. Each glass and glass-ceramic sample was pre-incubated in DMEM to give a glass-conditioned media that were added to the cell cultures for 1 and 3 days.

17

1   The PrestoBlue® viability data (Figure 4) showed that L929 cells in the presence either of glass- or

2   glass-ceramic-conditioned medium exhibited a metabolic activity higher than 50% for

3   concentrations lower than 50 mg/mL. In the case of BBG-Mg glass and glass-ceramics even after 3

4   days of culture, the cells displayed good metabolic activity for media conditioned by concentrations

5   of 50 mg/mL (e.g.: for BBG-Mg_ T_{c2} at 50 mg/mL concentration, cells present 74 % of metabolic

6   activity). However, all BBGs before and after heat treatment showed far higher metabolic activity

7   than the commercial 45S5 bioglass (e.g.: after 3 days of culture with 45S5 bioglass-conditioned

8   media, L929 cells showed only 1% of the metabolic activity observed in the control cultures).

9   Figure 5 exhibits the DNA measurements of L929 culture normalized to the control cultures

10   incubated in culture medium only. For all BBGs, before and after heat treatment, concentrations

11   below 50 mg/mL showed DNA levels indicating cell proliferation rates close to 100%, meaning that

12   the conditioned medium was not affecting cell proliferation. Similarly to the results observed in the

13   cell viability assays, BBG-Mg glass or glass-ceramics exhibited less cytotoxic effects than BBG-Ca

14   and -Sr glasses and glass-ceramics. Higher proliferation rates were observed with the media

15   conditioned with BBG-Mg than for the BBG-Ca or BBG-Sr-conditioned media (Figure 5).

16   Furthermore, culture medium conditioned by 45S5 bioglass was found to be significantly more

17   cytotoxic than culture medium conditioned with BBG glasses and glass-ceramics. Crystallisation of

18   the glasses was found to have no significant effect on cellular behaviour at day 1 however at day 3,

19   different cellular behaviour profiles were observed at all the concentrations tested. Specifically, for

20   the BBG-Mg glasses, an increase in cytotoxicity was detected for the first heat-treated glass-

21   ceramics (T_{c1}), which could be related to the formation of SiO_2 during the heat treatment. The

22   formation of SiO_2 molecules reduces the amount of silicate in the dominant amorphous phase,

23   which may increase the ratio of borate in the amorphous glass matrix. The borate-rich amorphous

24   phase has a faster degradation rate [15], increasing the quantity of ions in solution as well as the pH (~

25   8.0-9.0) [46]. On the other hand, the BBG-Mg glass-ceramics formed after the second heat treatment

26   (T_{c2}) showed a reduction in cytotoxic, which may have been due to the formation of two different

1 crystalline phases (magnesium silicate and magnesium borate) so reducing the availability of ions

2 contained largely within the stable crystalline phases [27, 30].

3 The glass-ceramics produced from heat-treated BBG-Ca and -Sr glasses also showed different

4 cellular behaviour from the parent glasses. A reduction in cytotoxicity was found for glass-ceramics

5 formed after the first heat treatment (T_{c1}) and an increase in cytotoxicity with further heat

6 treatments (T_{c2} and T_{c3}). These results may be explained by the formation of different crystalline

7 phases with higher availability for ion release, which may have increased the pH and can be directly

8 observed by colour changes in medium culture [30]. The pH of the non-conditioned and conditioned

9 media was measured and found to range from 8.0 to 8.5 for all BBG glasses and glass ceramics.

10 The pH of conditioned media from 45S5 bioglass ranged between 8.5 and 9. While the addition of

11 boron to glass matrix is associated with bone healing and formation as well higher conversion rates

12 to HA [6, 12]; the cytotoxic evaluation demonstrated that it is possible to modify the cytotoxic effects

13 of BBGs by a controlled crystallisation of the constituent glasses. Together, these features make

14 BBGs suitable candidates for bone tissue engineering application.
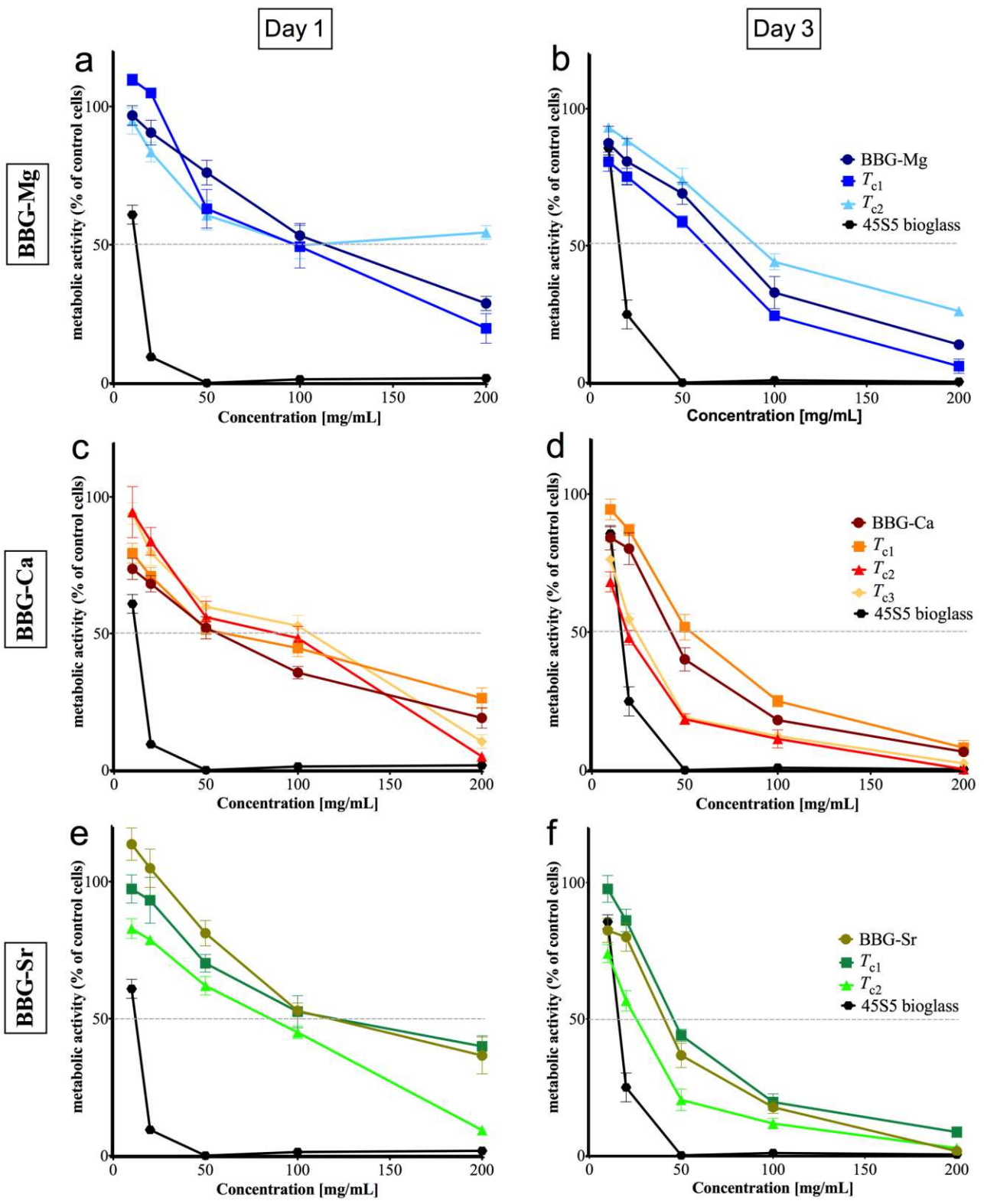
1

2 **Figure 4** - The cell viability of L929 cells after 1 and 3 days of culture with conditioned medium

3 from BBG-Mg, -Ca and -Sr glass and glass-ceramics. (a, c and e – 1 day of culture, b, d and f - 3

4 days of culture).

1
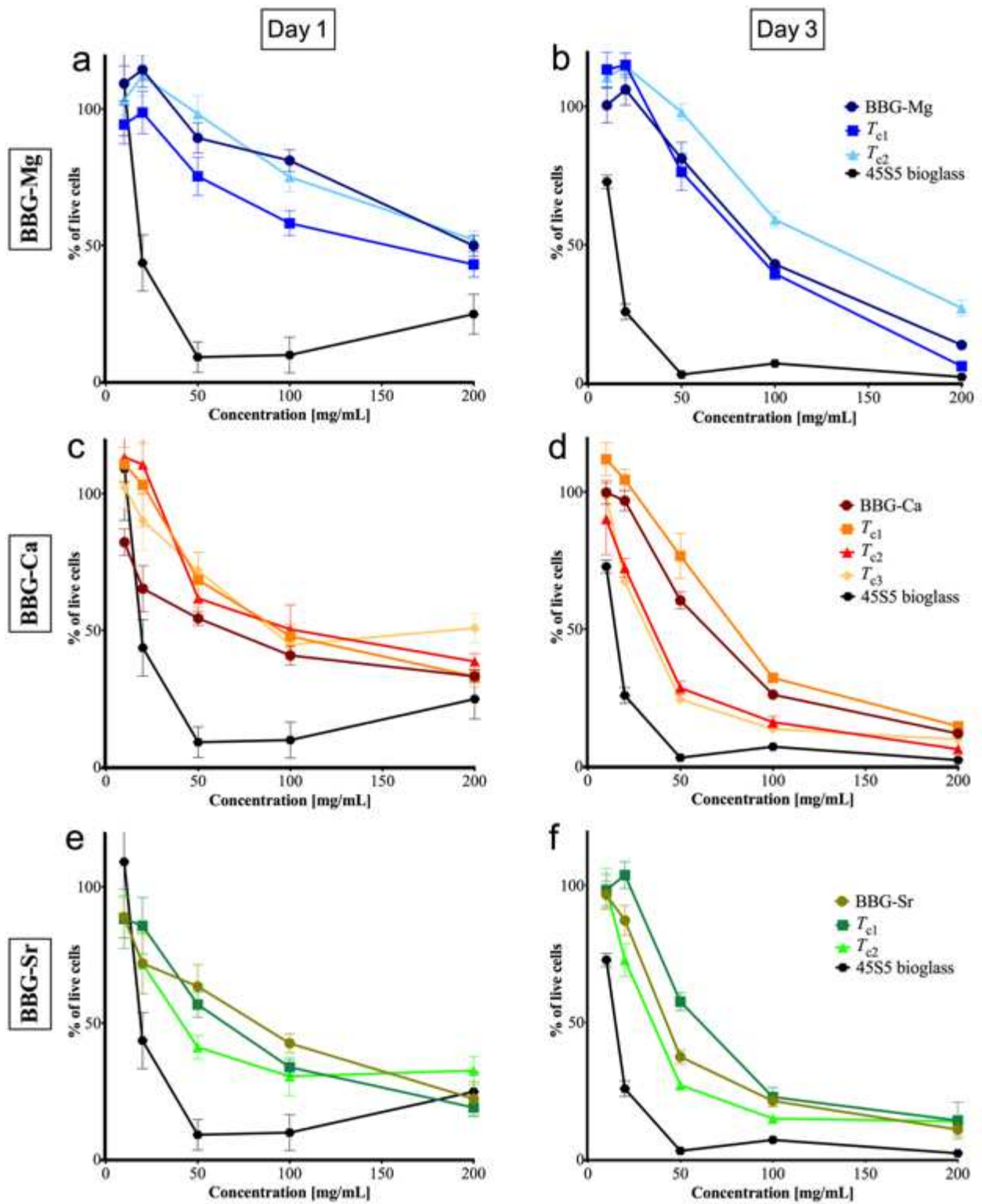
Figure 5 - The proliferation of L929 cells in contact with BBG-Mg, -Ca and -Sr glass and glass-

ceramic-conditioned media after 1 and 3 days of culture (a, c and 3 - after 1 day of culture, b, d and
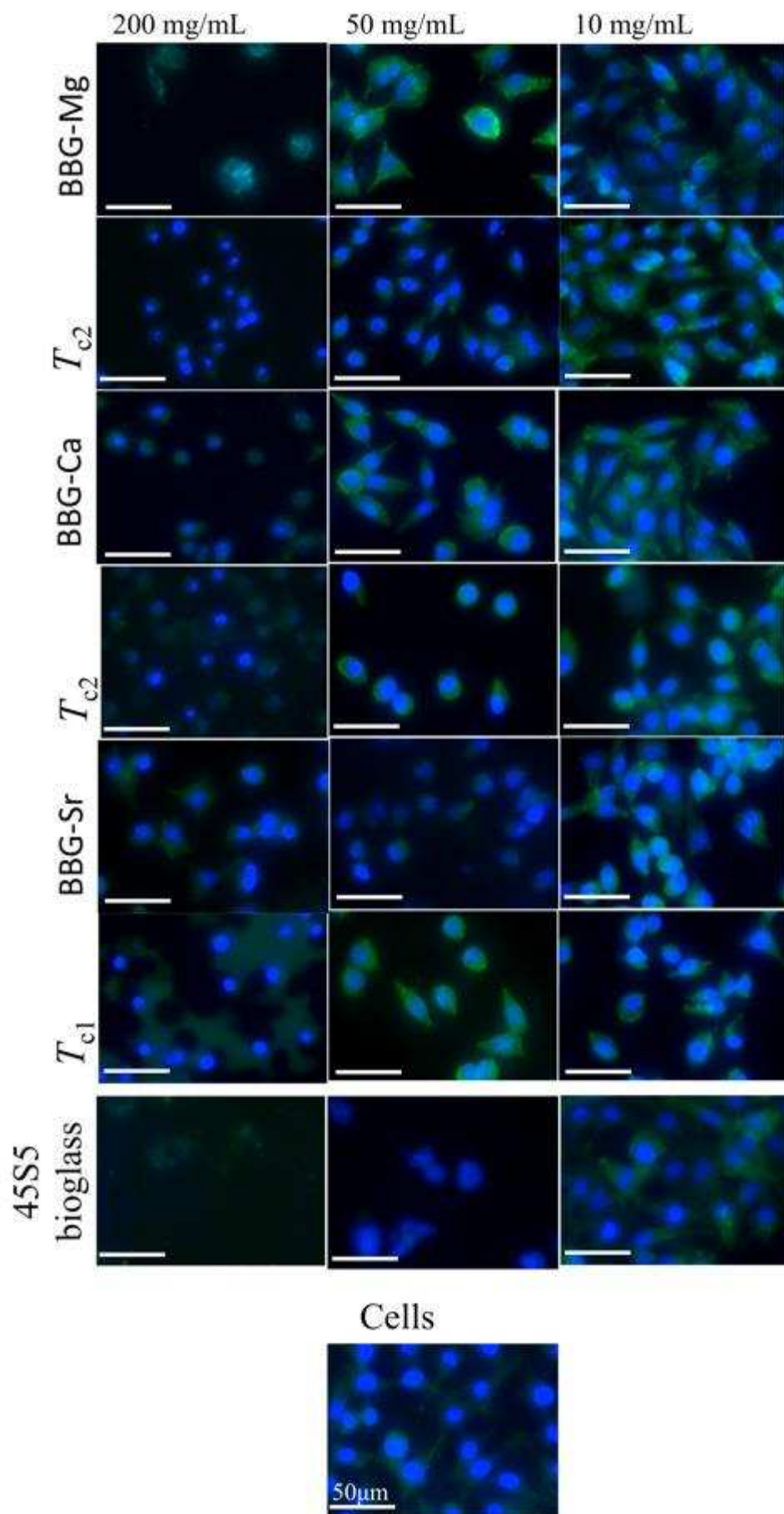
f - after 3 days of culture).

After 3 days of culture, morphologic assessment of L929 cells (Figure 6) revealed a concentration dependent behaviour of the BBG-Mg-, BBG-Ca- and BBGCs- conditioned media. Where of 10 mg/mL of BBG-Mg-, BBG-Ca-, BBG-Sr- or BBGCs were used to prepare the conditioned media, the cells, showed a characteristic fibroblast morphology with the formation of actin filaments that was similar to that of the control cultures in the absence of glass-conditioned media. Use of 50 mg/mL of BBG-Mg-, BBG-Ca- and BBG-Sr- and BBGCs to prepare the conditioned media, resulted in fewer cells with a classical elongated fibroblastic and a greater proportion exhibiting a more rounded morphology. Use of BBG-Mg-, BBG-Ca-, BBG-Sr- or BBGCs concentrations of 200 mg/mL gave conditioned media in which only a few rounded L929 cells could be observed after 3 days. These results are in agreement with cell viability and cell proliferation data (Figure 4 and 5) supporting a concentration dependence cytotoxic effect. In the case of the commercial 45S5 bioglass cultures, for concentrations higher than 10 mg/mL the in the conditioned media no live cells were observed after 3 days of culture. At lower 45S5 bioglass concentrations (10 mg/ml), culture of L929 cells in the 45S5 bioglass-conditioned media resulted in the cells having a fibroblastic morphology similar to the control cell cultures. As showed by the viability and the DNA assays, crystallisation of the glasses was found to have a positive or negative effect on cellular morphology at day 3 of culture. Especially for a concentration of 50 mg/ml, it was observed that the less toxic samples (i.e. BBG-Mg_Tc2, BBG-Ca_Tc1 and BBG-Sr_Tc1) presented higher number of cells with a classical elongated fibroblastic morphology. This is consistent with the typical lower solubility of the ceramic phases when compared to the glassy ones, limiting the release of ionic components from the BBGCs and maintaining them at non-cytotoxic concentrations in the culture medium.

Specifically, for the BBG-Mg glasses, an increase in cytotoxicity was detected for the first heat-treated glass-ceramics (T_{c1}), which could be related to the formation of SiO_2 during the heat treatment. The formation of SiO_2 molecules reduces the amount of silicate in the dominant amorphous phase, which may increase the ratio of borate in the amorphous glass matrix. The

1   borate-rich amorphous phase has a faster degradation rate [15], increasing the quantity of ions in

2   solution as well as the pH (~ 8.0-9.0) [46]. On the other hand, the BBG-Mg glass-ceramics formed

3   after the second heat treatment (T_{c2}) showed a reduction in cytotoxic, which may have been due to

4   the formation of two different crystalline phases (magnesium silicate and magnesium borate) so

5   reducing the availability of ions contained largely within the stable crystalline phases [27, 30].

6   The glass-ceramics produced from heat-treated BBG-Ca and -Sr glasses also showed different

7   cellular behaviour from the parent glasses. A reduction in cytotoxicity was found for glass-ceramics

8   formed after the first heat treatment (T_{c1}) and an increase in cytotoxicity with further heat

9   treatments (T_{c2} and T_{c3}). These results may be explained by the formation of different crystalline

10   phases with higher availability for ion release, which may have increased the pH and can be directly

11   observed by colour changes in the culture medium [30]. The pH of the non-conditioned and

12   conditioned media was measured and found to range from 8.0 to 8.5 for all BBG glasses and glass

13   ceramics. The pH of conditioned media from 45S5 bioglass ranged between 8.5 and 9.0.

14

1 **Figure 6** – Fluorescence microscopy of L929 cells morphology after 3 days incubation with BBGs

2 or BBGCs -conditioned media. Conditioned media were prepared with 10 mg/ml, 50 mg/ml or 200

3 mg/ml BBG glass or BBGCs. Cells cultured with non-conditioned medium was used as negative

4 control and 45S5 bioglass conditioned media was used as positive control (The blue colour (DAPI

5 staining) shows the nucleus of cells; Green colour (phalloidin staining) shows the actin filaments).

6 **4. Conclusions**

7 Three novel amorphous BBGs with different glass modifiers have been successfully synthesised by

8 the melt quench technique. The DTA analysis allowed the identification of two or more exothermic

9 peaks indicative of crystallisation. However, after a controlled heat treatment at these temperatures,

10 XRD and ATR-FTIR data indicated that only the samples that were treated at the higher

11 crystallisation temperatures produced significant crystalline phase(s). Also, different crystalline

12 phases were formed for the different substituted BBGs. Specifically for, BBG-Mg, BBG-Ca and

13 BBG-Sr glass-ceramics was detected the presence of magnesium silicate-$Mg_2(SiO_3)_2$ and

14 magnesium borate-$Mg_2B_2O_5$; wollastonite-2M-$CaSiO_3$ and calcium borate-$Ca(BO_2)_2$; and strontium

15 silicate-$SrSiO_3$ and strontium borate-$Sr_2B_2O_5$, respectively. To our knowledge, this is the first time

16 it is demonstrated that controlled crystallisation of BBGs might produce glass-ceramics with less

17 cytotoxic effects on cells. Moreover, neither BBGs nor BBGCs induced a cytotoxic effect on cells

18 at concentrations lower than 50 mg/mL and they exhibited less cytotoxicity compared to 45S5

19 bioglass at all concentrations used. Finally, interaction of BBGs with cells in a biological

20 environment is a complex process that is continuously under study from the scientific and medical

21 device communities. However, the great biodegradable properties of BBGs combined with the fact

22 that partial or total crystallisation permits cytotoxicity reduction. The BBGs can be used to achieve

23 medical-grade material for development of new generation bone tissue engineered implants.

Acknowledgements

References

(1)   El-Meliegy, E.; Van Noort, R., In Glasses and Glass Ceramics for Medical Applications. Springer **2012**.

(2)   Hench, L., The story of Bioglass. J. Mater. Sci.: Mater. Med. **2006,** 17, 967-978.

(3)   Bhakta, S.; Faira, P.; Salata, L.; de Oliveira Neto, P.; Miller, C.; van Noort, R.; Reaney, I.; Brook, I.; Hatton, P., Determination of relative in vivo osteoconductivity of modified potassium fluorrichterite glass–ceramics compared with 45S5 bioglass. J. Mater. Sci.: Mater. Med. **2012,** 23, 2521-2529.

(4)   Hench, L. L., Bioceramics: From Concept to Clinic. J. Am. Ceram. Soc. **1991,** 74, 1487-1510.

(5)   Fu, H.; Rahaman, M.; Day, D.; Huang, W., Long-term conversion of 45S5 bioactive glass–ceramic microspheres in aqueous phosphate solution. J. Mater. Sci.: Mater. Med. **2012,** 23, 1181-1191.

(6)   Xu, S.; Yang, X.; Chen, X.; Shao, H.; He, Y.; Zhang, L.; Yang, G.; Gou, Z., Effect of borosilicate glass on the mechanical and biodegradation properties of 45S5-derived bioactive glass-ceramics. J. Non-Cryst. Solids **2014,** 405, 91-99.

(7)   Rahaman, M. N.; Day, D. E.; Sonny Bal, B.; Fu, Q.; Jung, S. B.; Bonewald, L. F.; Tomsia, A. P., Bioactive glass in tissue engineering. Acta Biomater. **2011,** 7, 2355-2373.

(8)   Huang, W.; Day, D.; Kittiratanapiboon, K.; Rahaman, M., Kinetics and mechanisms of the conversion of silicate (45S5), borate, and borosilicate glasses to hydroxyapatite in dilute phosphate solutions. J. Mater. Sci.: Mater. Med. **2006,** 17, 583-596.

(9)   Brink, M.; Turunen, T.; Happonen, R.-P.; Yli-Urpo, A., Compositional dependence of bioactivity of glasses in the system Na2O-K2O-MgO-CaO-B2O3-P2O5-SiO2. J. Biomed. Mater. Res. **1997,** 37, 114-121.

(10)   Pan, H. B.; Zhao, X. L.; Zhang, X.; Zhang, K. B.; Li, L. C.; Li, Z. Y.; Lam, W. M.; Lu, W. W.; Wang, D. P.; Huang, W. H.; Lin, K. L.; Chang, J., Strontium borate glass: potential biomaterial for bone regeneration. J. R. Soc., Interface **2010,** 7, 1025-1031.

(11)   Rahaman, M. N.; Liang, W.; Day, D. E., Preparation and Bioactive Characteristics of Porous Borate Glass Substrates. In Advances in Bioceramics and Biocomposites: Ceram. Eng. Sci. Proc., John Wiley & Sons, Inc.: 2008; 1-10.

(12)   Lakhkar, N. J.; Lee, I.-H.; Kim, H.-W.; Salih, V.; Wall, I. B.; Knowles, J. C., Bone formation controlled by biologically relevant inorganic ions: Role and controlled delivery from phosphate-based glasses. Adv. Drug Delivery Rev. **2013,** 65, 405-420.

(13)   Shen, Y.; Liu, W.; Wen, C.; Pan, H.; Wang, T.; Darvell, B. W.; Lu, W. W.; Huang, W., Bone regeneration: importance of local pH-strontium-doped borosilicate scaffold. J. Mater. Chem. **2012,** 22, 8662-8670.

(14)   Chapin, R.; Ku, W.; Kenney, M.; McCoy, H., The effects of dietary boric acid on bone strength in rats. Biol. Trace Elem. Res. **1998,** 66, 395-399.

(15)   Yang, X.; Zhang, L.; Chen, X.; Sun, X.; Yang, G.; Guo, X.; Yang, H.; Gao, C.; Gou, Z., Incorporation of B2O3 in CaO-SiO2-P2O5 bioactive glass system for improving strength of low-temperature co-fired porous glass ceramics. J. Non-Cryst. Solids **2012,** 358, 1171-1179.

(16)   Ciceo Lucacel, R.; Radu, T.; Tătar, A. S.; Lupan, I.; Ponta, O.; Simon, V., The influence of local structure and surface morphology on the antibacterial activity of silver-containing calcium borosilicate glasses. J. Non-Cryst. Solids **2014,** 404, 98-103.

(17)   Wang, H.; Zhao, S.; Xiao, W.; Cui, X.; Huang, W.; Rahaman, M. N.; Zhang, C.; Wang, D., Three-dimensional zinc incorporated borosilicate bioactive glass scaffolds for rodent critical-sized calvarial defects repair and regeneration. Colloids Surf., B **2015,** Jun 1, 149-56.

(18)   Baino, F.; Minguella, J.; Kirk, N.; Montealegre, M. A.; Fiaschi, C.; Korkusuz, F.; Orlygsson, G.; Chiara, V.-B., Novel full-ceramic monoblock acetabular cup with a bioactive trabecular coating: design, fabrication and characterization. Ceram. Int. **2016,** 42, 6833-6845.

(19)   Fu, Q.; Rahaman, M. N.; Bal, B. S.; Bonewald, L. F.; Kuroki, K.; Brown, R. F., Silicate, borosilicate, and borate bioactive glass scaffolds with controllable degradation rate for bone tissue engineering applications. II. In vitro and in vivo biological evaluation. J. Biomed. Mater. Res., Part A| Oct 2010 **2010,** 95A.

(20)   Rahaman, M. N., In Tissue Engineering Using Ceramics and Polymers (Second Edition), Boccaccini, A. R.; Ma, P. X., Eds. Woodhead Publishing, 2014; Chapter 3, 67-114.

(21)   Wu, C.; Fan, W.; Gelinsky, M.; Xiao, Y.; Simon, P.; Schulze, R.; Doert, T.; Luo, Y.; Cuniberti, G., Bioactive SrO–SiO2 glass with well-ordered mesopores: Characterization, physiochemistry and biological properties. Acta Biomater. **2011,** 7, 1797-1806.

(22)   Hoppe, A.; Güldal, N. S.; Boccaccini, A. R., A review of the biological response to ionic dissolution products from bioactive glasses and glass-ceramics. Biomaterials **2011,** 32, 2757-2774.

(23)   Santocildes-Romero, M. E.; Crawford, A.; Hatton, P. V.; Goodchild, R. L.; Reaney, I. M.; Miller, C. A., The osteogenic response of mesenchymal stromal cells to strontium-substituted bioactive glasses. J. Tissue Eng. Regener. Med. **2015,** 9, 619-631.

(24)   Yamasaki, Y.; Yoshida, Y.; Okazaki, M.; Shimazu, A.; Uchida, T.; Kubo, T.; Akagawa, Y.; Hamada, Y.; Takahashi, J.; Matsuura, N., Synthesis of functionally graded MgCO3 apatite accelerating osteoblast adhesion. J. Biomed. Mater. Res. **2002,** 62, 99-105.

(25)   Maeno, S.; Niki, Y.; Matsumoto, H.; Morioka, H.; Yatabe, T.; Funayama, A.; Toyama, Y.; Taguchi, T.; Tanaka, J., The effect of calcium ion concentration on osteoblast viability, proliferation and differentiation in monolayer and 3D culture. Biomaterials **2005,** 26, 4847-4855.

(26)   Marie, P. J.; Ammann, P.; Boivin, G.; Rey, C., Mechanisms of Action and Therapeutic Potential of Strontium in Bone. Calcif. Tissue Int. **2001,** 69, 121-129.

(27)   Daguano, J. K. M. F.; Strecker, K.; Ziemath, E. C.; Rogero, S. O.; Fernandes, M. H. V.; Santos, C., Effect of partial crystallization on the mechanical properties and cytotoxicity of bioactive glass from the 3CaO.P2O5–SiO2–MgO system. J. Mech. Behav. Biomed. Mater. **2012,** 14, 78-88.
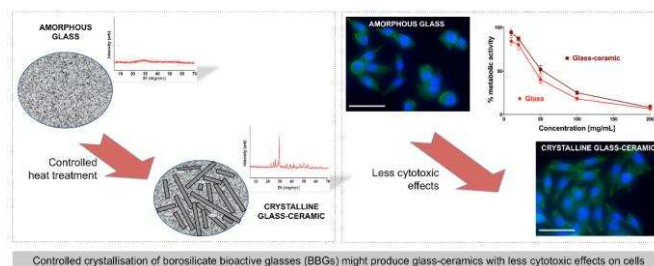
(28)   Cao, J.; Wang, Z., Effect of Na2O and heat-treatment on crystallization of glass–ceramics from phosphorus slag. J. Alloys Compd. **2013,** 557, 190-195.

(29)   Wu, L.; Li, Y.; Teng, Y.; Meng, G., Preparation and characterization of borosilicate glass-ceramics containing zirconolite and titanite crystalline phases. J. Non-Cryst. Solids **2013,** 380, 123-127.

(30)   Hurrell-Gillingham, K.; Reaney, I. M.; Miller, C. A.; Crawford, A.; Hatton, P. V., Devitrification of ionomer glass and its effect on the in vitro biocompatibility of glass-ionomer cements. Biomaterials **2003,** 24, 3153-3160.

(31)   Baino, F.; Marshall, M.; Kirk, N.; Vitale-Brovarone, C., Design, selection and characterization of novel glasses and glass-ceramics for use in prosthetic applications. Ceram. Int. **2016,** 42, 1482-1491.

(32)   Venkateswara Rao, G.; Shashikala, H. D., Effect of heat treatment on optical, dielectric and mechanical properties of silver nanoparticle embedded CaOCaF2P2O5 glass. J. Alloys Compd. **2015,** 622, 108-114.

(33)   Freeman, C. O.; Brook, I. M.; Johnson, A.; Hatton, P. V.; Hill, R. G.; Stanton, K. T., Crystallization modifies osteoconductivity in an apatite–mullite glass–ceramic. J. Mater. Sci.: Mater. Med. **2003,** 14, 985-990.

(34)   ISO/EN10993–5, Biological Evaluation of Medical Devices - Part 5: Tests for Cytotoxicity: In Vitro Methods. Geneva, Switzerland: International Standards **1992**.

(35)   Schaut, R. A., The Effect of Boron Oxide on the Composition, Structure, and Adsorptivity of Glass Surfaces. Ph.D. Thesis, The Pennsylvania State University, U.S.A. **2008**.

(36)   Gautam, C. R.; Kumar, D.; Parkash, O.; Singh, P., Synthesis, IR, crystallization and dielectric study of (Pb, Sr)TiO 3 borosilicate glass–ceramics. Bull. Mater. Sci. **2013,** 36, 461-469.

(37)   Echezarreta-López, M. M.; De Miguel, T.; Quintero, F.; Pou, J.; Landin, M., Antibacterial properties of laser spinning glass nanofibers. Int. J. Pharm. **2014,** 477, 113-121.

(38)   Efimov, A. M.; Pogareva, V. G., IR absorption spectra of vitreous silica and silicate glasses: The nature of bands in the 1300 to 5000 cm−1 region. Chem. Geol. **2006,** 229, 198-217.

(39)   Serra, J.; González, P.; Liste, S.; Serra, C.; Chiussi, S.; León, B.; Pérez-Amor, M.; Ylänen, H. O.; Hupa, M., FTIR and XPS studies of bioactive silica based glasses. J. Non-Cryst. Solids **2003,** 332, 20-27.

(40)   Husung, R. D.; Doremus, R. H., The infrared transmission spectra of four silicate glasses before and after exposure to water. J. Mater. Res. **1990,** 5, 2209-2217.

(41)   Dunken, H.; Doremus, R. H., Short time reactions of a na2o-cao-sio2 glass with water and salt solutions. J. Non-Cryst. Solids **1987,** 92, 61-72.

(42)   Goh, Y.-F.; Alshemary, A. Z.; Akram, M.; Abdul Kadir, M. R.; Hussain, R., In-vitro characterization of antibacterial bioactive glass containing ceria. Ceram. Int. **2014,** 40, 729-737.

(43)   Doweidar, H.; Zeid, M. A. A.; El-Damrawy, G. M., Effect of gamma radiation and thermal treatment on some physical properties of ZnO-PbO-B 2 O 3 glasses. J. Phys. D: Appl. Phys. **1991,** 24, 2222.

(44)   Singh, S.; Singh, A.; Bhatti, S. S., Elastic moduli of some mixed alkali borate glasses. J. Mater. Sci. **1989,** 24, 1539-1542.

(45)   Tenney, A. S.; Wong, J., Vibrational Spectra of Vapor - Deposited Binary Borosilicate Glasses. The J. Chem. Phys. **1972,** 56, 5516-5523.

(46)   Teo, A.; Mantalaris, A.; Lim, M., Influence of culture pH on proliferation and cardiac differentiation of murine embryonic stem cells. Biochem. Eng. J. **2014,** 90, 8-15.

The Design and Properties of Novel Substituted Borosilicate Bioactive Glasses and Their Glass-Ceramic Derivatives

João S. Fernandes, Piergiorgio Gentile, Robert Moorehead, Aileen Crawford, Cheryl Miller, Ricardo A. Pires, Paul V. Hatton, Rui L. Reis

Controlled crystallisation of borosilicate bioactive glasses (BBGs) might produce glass-ceramics with less cytotoxic effects on cells

With this research the effect of crystallisation on the properties of borosilicate bioactive glasses (BBGs) and their suitability as biomaterials was evaluated. By in vitro cytotoxicity assay we demonstrated that the crystallisation of the BBGs reduced their cytotoxicity to L929 cell line, providing a method for the improvement of the biocompatibility of bioactive borosilicate glass-ceramics.